

# Personalized analysis of minimal residual cancer cells in peritoneal lavage fluid predicts peritoneal dissemination of gastric cancer

**Dongbin Zhao**

Chinese Academy of Medical Sciences and Peking Union Medical College

**Pinli Yue**

Chinese Academy of Medical Sciences and Peking Union Medical College

**Tongbo Wang**

National Cancer Center/National Clinical Research Center for Cancer/Cancer Hospital, Chinese Academy of Medical Sciences and Peking Union Medical College

**Pei Wang**

Chinese Academy of Medical Sciences and Peking Union Medical College

**Qianqian Song**

Chinese Academy of Medical Sciences and Peking Union Medical College

**Jingjing Wang**

Jinchenjunchuang Clinical Laboratory

**Yuchen jiao** (✉ [jiaoyuchen@126.com](mailto:jiaoyuchen@126.com))

Chinese Academy of Medical Sciences and Peking Union Medical College <https://orcid.org/0000-0001-7917-8810>

---

## Article

**Keywords:** Gastric Cancer, Peritoneal lavage fluid, Peritoneal dissemination, Personalized mutation assay, Minimal residual disease

**Posted Date:** March 10th, 2021

**DOI:** <https://doi.org/10.21203/rs.3.rs-275520/v1>

**License:** © ⓘ This work is licensed under a Creative Commons Attribution 4.0 International License.

[Read Full License](#)

---



22 **ABSTRACT**

23 Peritoneal dissemination (PD) is the major type of gastric cancer (GC) recurrence and leads to  
24 rapid death. Current approach cannot precisely determine which patients are at high risk of PD.  
25 In this study, we developed a technology to detect minimal residual cancer cells in peritoneal  
26 lavage fluid (PLF) samples by parallel profiling tumor-specific mutations. We applied the  
27 technology to a prospective cohort of 110 GC patients. The technology showed ultra-high  
28 sensitivity by successfully detecting all the 27 cases that developed PD. The minimal residual  
29 cancer cells in PLF was associated with an increased risk of PD (HR = 145.13; 95%CI =  
30 20.20-18435.79;  $p < 0.001$ ) and significantly shorter overall survival. In pathologically high-risk  
31 (T4) patients, the PLF mutation profiling model exhibited even greater specificity of 91% and  
32 positive predictive value of 88%, while retaining sensitivity of 100%. PLF cancer cell fraction  
33 remained the strongest independent predictor of PD and recurrence-free survival over  
34 pathologic diagnosis and cytological diagnosis in GC patients. This approach may help in the  
35 postsurgical management of GC patients by detecting PD far before the metastatic lesions  
36 grow to significant size detectable by conventional methods such as MRI and CT scanning.

37

38 **Key words:** Gastric Cancer; Peritoneal lavage fluid; Peritoneal dissemination; Personalized  
39 mutation assay; Minimal residual disease

40

41 **INTRODUCTION**

42 Gastric Cancer (GC) is the fifth most common and the third leading cause of cancer death in  
43 the world<sup>1</sup>. Peritoneal dissemination (PD) is the most common form of GC recurrence and a  
44 strong indicator of poor prognosis with a 13% overall 5-year survival rate<sup>2</sup>. Although multiple  
45 therapeutic solutions, such as hyperthermic intraperitoneal chemotherapy (HIPEC) and  
46 extensive intraoperative peritoneal lavage plus intraperitoneal chemotherapy (EIPL-IPC), have  
47 been developed as prophylactic strategies targeting PD<sup>3,4</sup>, the preventive effect is  
48 compromised due to the difficulty to precisely identify the patients who will develop PD. Many  
49 studies have demonstrated that HIPEC and IPC could effectively prevent PD and improve the  
50 survival rate of patients with advanced gastric cancer<sup>5-7</sup>. However, once the peritoneal  
51 metastasis reaches a stage detectable by imaging, subsequent chemotherapy is not effective  
52 because of the complex intraperitoneal environment, and the advanced PD leads to many  
53 complications and rapid death (5-16 months)<sup>8-11</sup>. Thus, prediction or early detection of PD  
54 would help identify the GC patients who need intensive therapy to prevent PD.

55 Several studies shed light on the prediction of PD by the detection of cancer cells in  
56 peritoneal lavage fluid (PLF) samples<sup>12</sup>. Previous studies of peritoneal metastasis focused on  
57 conventional cytology. However, the sensitivity to detect minimal residual cancer cells to  
58 predict PD reached no more than 30%<sup>13-15</sup>. With the development of reverse transcriptase  
59 PCR (RT-PCR) technology, several studies began to examine cancer tissue specific  
60 messenger RNAs (mRNA) in PLF, such as carcinoembryonic antigen (CEA)<sup>16-18</sup>,  
61 cytokeratin-20 (CK-20)<sup>19</sup>, and matrix metalloproteinase-7 (MMP-7)<sup>20</sup>. None of these mRNAs is  
62 an ideal marker due to low sensitivity or specificity. The main source of such results is thought

63 to be the amplification of low-level CEA from peritoneal inflammatory cells, and the aberrant  
64 expression of mRNA originating from granulocytes<sup>21</sup>. In recent years, there have been several  
65 minimal residual disease (MRD) studies using exosomes and methylation to predict PD<sup>22,23</sup>.  
66 Some studies detected MRD by profiling GC-specific methylation alterations with bisulfite  
67 treatment and qPCR<sup>24,25</sup>. The clinical application of such MRD detection from PLF is limited  
68 primarily for two reasons. First, GC is a highly heterogeneous disease, rendering it difficult to  
69 identify highly tumor-specific and prevalent biomarkers among all GC cases. Second, the ratio  
70 of residual cancer cells among normal cells in PLF can be very low and undetectable with  
71 standard qPCR-based methods.

72       Recent developments in next generation sequencing (NGS) enable genome-wide  
73 profiling of tumor tissues to identify somatic mutations which are highly tumor-specific  
74 biomarkers to track MRD<sup>26</sup>. With recent developments in experimental and bioinformatic  
75 technologies, high throughput sequencing can also be applied to detect low frequency  
76 mutations in cell free DNA (cfDNA), providing a basis to improve MRD detection with high  
77 sensitivity<sup>27</sup>. Several recent studies have profiled tumor samples for somatic mutations and  
78 tracked the mutations in the cfDNA from matched blood samples to detect MRD<sup>28-31</sup>. The  
79 mutation-based MRD detection showed strong performance in the prediction of recurrence in  
80 multiple tumor types.

81       In this study, we applied Mutation Capsule, a mutation profiling technology, to profile up to  
82 20 mutations on the genomic DNA of cell pellets of PLF samples collected after abdominal  
83 exploration and before any manipulation of the stomach. We developed a model to evaluate  
84 the fraction of cancer cells among normal cells based on the number, fraction and sequencing

85 depth of the mutations detected. The assay precisely predicted all PD cases with 100%  
86 sensitivity, 85% specificity, 71% positive predictive value (PPV) and 100% negative predictive  
87 value (NPV). For stage T4 GC patients, the approach exhibited higher specificity (91%) and  
88 PPV (88%), with sensitivity and NPV at 100%.

89 To our knowledge, this study is the first to apply the personalized and mutation-based  
90 assay to profile MRD in cells pelleted from PLF. Our study demonstrates that PLF cancer cell  
91 fraction is a powerful biomarker for prognosis and early detection of PD.

92

93 **RESULTS**

94 **Patient enrollment and study design**

95 A total of 110 patients with stages I to III GC (mean [SD] age, 61 [9.6] years; 79 [76%] male)  
96 were enrolled in the study. Six patients were excluded from the study for palliative surgery ( $n =$   
97 4) or the presence of other types of cancer ( $n = 2$ ). Finally, a total of 104 patients were included  
98 in the analysis (Fig. 1). Recurrence of PD was defined as lesions detected in one of the  
99 following ways: MRI, CT scan, PET-CT scan visualized [ $^{18}\text{F}$ ]fluorodeoxyglucose ( $^{18}\text{F}$ -FDG)  
100 uptake over peritoneum and bowel with or without ascites >50 mL, or tumor cells detected in  
101 ascites or biopsy of peritoneal lesions. The median follow-up period was 20 months (6-41  
102 months). Clinicopathological characteristics of the 104 patients are listed in Supplementary  
103 Table 1. Surgery consisted of a radical resection of the primary tumor and at least D2 lymph  
104 node dissection.

105 We performed exome sequencing on the DNA from tumor tissue and matched white blood  
106 cell (WBC) samples to identify somatic mutations. A median of 101 mutations were detected in  
107 the primary tumor samples of each patient. We designed customized primers to profile up to  
108 20 somatic mutations in the peritoneal lavage samples with the Mutation Capsule technology  
109 (Supplementary Table 2)<sup>32</sup>.

110

111 **Construction and validation of the cancer cell fraction model**

112 Due to the low fraction of residual cancer cells among normal cells in PLF, the number of  
113 molecules present for a given mutation site in the sequencing (distinct coverage) might be  
114 insufficient to precisely detect the mutation. Thus, the detected frequency of one mutation

115 might not precisely represent the ratio of cancer cells<sup>33,34</sup>. Here, we set up a model to estimate  
116 the cancer cell ratio based on allele frequency and sequencing depth of somatic mutations in  
117 tumor tissue and paired PLF samples (Fig. 2a). For each traced somatic mutation, we  
118 determined the mutation frequency in the PLF sample and compared with the frequency in the  
119 primary tumor. The sample-level estimated cancer cell fraction was determined with the  
120 Maximum Likelihood Estimation.

121 To validate the accuracy of the cancer cell fraction model, we serially diluted cells from the  
122 cell line PLC/PRF/5 with cells from a second cell line A549 to generate 9 dilutions (PLC/PRF/5  
123 cell fraction = 0%, 0.0001%, 0.0003%, 0.001%, 0.005%, 0.05%, 0.5%, 5% and 33%). We  
124 selected 20 unique SNPs in PLC/PRF/5, and designed a customized assay targeting the  
125 SNPs. In each diluted sample, we profiled the 20 SNPs to calculate the estimated dilution ratio  
126 with the model (Supplementary Table 3). The data exhibited a strong linear correlation  
127 between the theoretical and estimated dilution ratios up to the dilution of 1:100,000 ( $R^2 =$   
128 0.9998) (Fig. 2b). Background noise observed at 0% PLC/PRF/5 cell input was 0.0007%  
129 (maximum value) among the 20 independent replicates (Fig. 2c). Based on the analytical  
130 validation results, the cancer cell fraction model exhibited 100% sensitivity at 0.001% spiked-in  
131 cell fraction, 67% sensitivity at 0.0003% cell fraction, and 33% sensitivity at 0.0001% cell  
132 fraction (Supplementary Table 4 and Supplementary Fig. 1). The data indicated a limit of  
133 detection (LOD) at a 0.001% cancer cell fraction based on the multi target site model.

134 To evaluate the biological noise of random mutations from non-tumor cells in PLF  
135 samples, we determined the fraction of 20 mutations that were not detected in the matched  
136 tumor sample. We calculated a set of cancer cell fractions based on these non-tumor-specific

137 mutations, and found the fractions from background noise in all PLF samples to be lower than  
138 0.01% (Fig. 2d, mean = 0.0006%, maximum = 0.0082%). To achieve a high specificity, we  
139 classified the cancer cell fraction as positive or negative with a cutoff of 0.01% in further  
140 analyses.

141

### 142 **Association of peritoneal lavage cancer cell fraction with risk of peritoneal** 143 **dissemination**

144 For the 104 patients, we chose a total of 1,717 mutations in the analysis (Supplementary Table  
145 5). On average, 17 somatic mutations (3-23 mutations per person) were tracked for each  
146 patient (Fig. 3a), and 25.7% (441/1,717) of the tracked mutations were detected in matched  
147 PLF samples. We calculated the cancer cell fraction based on the frequency and distribution of  
148 the tracked mutations with the model. The cancer cell fraction ranged from 0 to 23.41% (mean  
149 0.48%, median 0.0074%). Forty-two out of the 104 (40%) patients were positive ( $\geq 0.01\%$   
150 cancer cell fraction in PLF sample), and 62 (60%) were negative in the PLF mutation profiling  
151 model (Fig. 3a and Supplementary Table 6). Among the 104 patients, 27 patients experienced  
152 peritoneal dissemination, and all (27/27, 100%) of them tested positive in the PLF mutation  
153 profiling model. Six patients developed lymphatic metastasis, and 4 (67%) tested positive in  
154 the PLF mutation profiling model. In addition, 15% (11/71) of the non-recurrence patients were  
155 positive. The differences in cancer cell fraction between recurrence and non-recurrence  
156 groups were significant (PD, mean [SD], 0.0169 [0.04706] versus non-recurrence, mean [SD],  
157 0.0004 [0.00294],  $p < 0.001$ ; lymphatic metastasis, mean [SD], 0.0020 [0.00433] versus  
158 non-recurrence, mean [SD], 0.0004 [0.00294],  $p = 0.013$ ) (Fig. 3b).

159 Patients that were positive in the PLF mutation profiling model showed an increased risk  
160 of PD (HR = 145.13; 95%CI = 20.20-18435.79;  $p < 0.001$ ) (Fig. 4a). Twenty-seven of the 38  
161 (71%) test-positive patients and none of the 60 (0%) test-negative patients experienced PD.  
162 Kaplan-Meier estimates of recurrence free interval (RFI) at 3 years for test-positive patients  
163 were 17.60% (95%CI = 0%-35.24%), and for test-negative patients, 100%. In receiver  
164 operating characteristic (ROC) analysis, cancer cell fraction (AUC = 0.92) achieved 100%  
165 sensitivity and 85% specificity, with a PPV of 71% (Table 1).

166

#### 167 **Comparison of the cancer cell fraction and clinical risk factors on the prediction of PD**

168 We further compared the predictive value of the PLF mutation profiling model with clinical risk  
169 factors including cytological diagnosis and pathologic diagnosis, which was defined as high  
170 (T4) or low (T0-3) according to the standard criteria. The RFI outcomes of cytological and  
171 pathologic diagnosis risk assessments were the following, respectively: HR = 4.92; 95%CI =  
172 2.10-11.51;  $p < 0.001$  (Supplementary Fig. 2a); and HR = 5.04; 95%CI = 1.74-14.58;  $p = 0.001$   
173 (Supplementary Fig. 2b). Cytological diagnosis exhibited high specificity (94%, 67/71) but low  
174 sensitivity (30%, 8/27). On the other hand, pathologic diagnosis showed high sensitivity (85%,  
175 23/27) but low specificity (54%, 38/71) (Table 1). The performance of cytological diagnosis and  
176 pathologic diagnosis were consistent with previous reports<sup>35-37</sup>.

177 Interestingly, we found that 8 of the 11 false positive cases by the PLF mutation profiling  
178 model occurred in stage T1-3 cases, while only 4 cases in this group developed PD. Among  
179 the pathologically high-risk patients of stage T4 ( $n = 56$ ), the PLF mutation profiling model  
180 exhibited a lower false positive rate, delivering 100% (23/23) sensitivity, 91% (30/33) specificity,

181 and 88% (23/26) PPV. The RFI outcomes of PLF cancer cell fraction assessment in stage T4  
182 cases was HR = 132.43; 95%CI = 17.55-17006.37;  $p < 0.001$  (Fig. 4b).

183 To adjust for multiple variables in a single model, we used a cox proportional hazard  
184 model. PLF cancer cell fraction remained the strongest independent predictor of  
185 recurrence-free survival (RFS) (HR = 141.27, 95%CI = 17.37-18633.39;  $p < 0.001$ ), followed  
186 by pathologic diagnosis (HR = 3.82, 95%CI = 1.21-17.27;  $p = 0.02$ ) (Supplementary Table 7).

187

### 188 **Prediction of recurrence with the PLF mutation profiling model**

189 Six of the 104 patients experienced lymphatic metastasis during the 41-month follow-up. Of  
190 these 6 samples, 4 were positive in the PLF mutation profiling test. When we combined  
191 peritoneal dissemination and lymphatic metastasis patients as a recurrence group, the  
192 test-positive patients by the PLF mutation profiling model were 40 times more likely to relapse  
193 than the test-negative patients (HR = 39.97; 95%CI = 9.50-168.10;  $p < 0.001$ ) (Supplementary  
194 Fig. 2c). Kaplan-Meier estimates of RFI at 3 years for test-positive patients was 15.80% (95%  
195 CI = 0%-31.68%), and for those test-negative was 96.50% (95% CI = 91.80%-100%). The PLF  
196 mutation profiling model achieved 94% (31/33) sensitivity, 85% (60/71) specificity, 74% (31/42)  
197 PPV and 97% (60/62) NPV (Table 1).

198 During the follow-up period, 10 patients had developed disease recurrence and died from  
199 metastatic disease, and all of them were test-positive in the PLF mutation profiling model. A  
200 significantly shorter overall survival (OS) was associated with a positive result in the model  
201 (HR = 50.35; 95%CI = 6.41-6492.15;  $p < 0.001$ ) (Figure 4C). The median survival of these 10  
202 patients was 22 months (6-39 months).

203 **DISCUSSION**

204 PD accounts for 50% of recurrence in GC patients and is associated with exceptionally poor  
205 prognosis<sup>38</sup>. CT and other imaging modalities are used to diagnose PD, but the sensitivity to  
206 predict or detect PD in early and curable stage is inadequate as such metastatic lesions could  
207 be small and easily missed. When GC patients show PD-associated symptoms such as  
208 ascites and intestinal obstruction, or when metastases can be observed by imaging, the PD  
209 lesions are often in significant size and advanced stage, with no effective treatments available.  
210 In addition to peritoneal cytology, multiple biomarkers including mRNA, methylation and  
211 protein markers have been used to profile PLF to predict PD among GC patients<sup>39-41</sup>. However,  
212 the accuracy of these approaches for the early detection of PD is still limited<sup>13,42</sup>. A potential  
213 reason is that GC is a highly heterogeneous disease, rendering it difficult to find a marker  
214 suitable for all GC cases. In addition, the fraction of cancer cells among PLF cell pellets could  
215 be very low and beyond the limit of detection.

216 MRD detection based on a customized assay targeting tumor-specific mutations in  
217 plasma cfDNA have shown promising performance in prognostic prediction and disease  
218 monitoring in several tumor types, including breast, colorectal and lung cancers<sup>28,30,43</sup>. Other  
219 non-blood samples have also been used for specific clinical scenarios. For example, cell  
220 pellets in urine have been used to monitor the development of bladder cancers<sup>44</sup>. In this study,  
221 we developed a customized assay to profile up to 20 tumor-specific mutations in PLF DNA.  
222 We also set up a model to evaluate the fraction of cancer cells. Using a standard reference of  
223 mixed cancer cell lines, we found that the approach confidently detected cancer cells when the  
224 fraction was as low as 0.001%. In clinical PLF samples, the biological noise was close to

225 0.01%, possibly due to random mutations in epithelial cells or white blood cells<sup>45</sup>.

226 We applied the pipeline to detect MRD in PLF samples from GC patients. The approach  
227 exhibited a strong performance in the prediction of PD with 100% sensitivity, 85% specificity  
228 and 71% PPV. The sensitivity of the mutation profiling model is higher than that of peritoneal  
229 cytology or pathology based on a direct comparison in the same cohort. Mutation profiling also  
230 exhibited increased performance relative to other previously reported PLF-based detection  
231 assays<sup>46-48</sup>. Furthermore, the combination with clinical risk factors (stage T4) further improved  
232 the performance. In the subgroup of T4 high risk individuals, the mutation profiling model  
233 showed an even stronger performance with 100% sensitivity, 91% specificity and 88% PPV.  
234 Therefore, the PLF mutation profiling should be especially helpful for stage T4 patients to  
235 predict the development of PD. An interventional clinical trial targeting T4 and  
236 PLF-mutation-positive patients might answer the question as to whether intensive  
237 post-operational treatment targeting PD might help to prevent recurrence and improve overall  
238 survival.

239 Our study suggests that mutation-based MRD profiling in PLF samples is effective in  
240 predicting PD at the time of surgery, especially in stage T4 patients.

241

242 **METHODS**

243 **Patients and samples**

244 From June, 2017, to December, 2019, 110 gastric cancer patients scheduled for surgery in  
245 National Cancer Center, Cancer Hospital, Chinese Academy of Medical Sciences, were  
246 enrolled in our study. Eligibility criteria of the study included a diagnosis of stage I to III  
247 resectable gastric cancer determined by chest-abdominal-pelvic enhanced computed  
248 tomography-scan (CT-scan), MRI or upper gastrointestinal endoscopy ± endoscopic  
249 ultrasound (EUS); no metastatic disease evident on staging computed tomography (CT); age  
250 < 80 years; no preoperative radiotherapy or chemotherapy; and a treatment plan for resection.  
251 In accordance with NCCN guidelines, postoperative chemotherapy was recommended after  
252 surgery. Patients with another malignant neoplasm diagnosed within the last 3 years were  
253 excluded. After therapy, surveillance was performed according to the standard of care, with  
254 clinical assessment every 3 months for the first 2 years and every 6 months for the next years.  
255 TNM stages were determined according to the 8th edition of the Union for International Cancer  
256 Control.

257 For collection of PLF samples, 300-400 mL of normal saline was used to wash the upper  
258 abdominal cavity after abdominal exploration and before any manipulation of the tumor during  
259 surgery. A total of 200 mL of PLF was collected. PLF (100 mL) was examined through  
260 conventional cytological diagnosis with Papanicolaou and Giemsa staining. The remaining 100  
261 mL of PLF was used in mutation profiling. PLF samples were centrifuged first at 2500 rpm  
262 (1098g) for 10 min to remove the supernatant, and further centrifuged at 12,000 rpm for 10 min  
263 to obtain the PLF pellet. Blood samples were collected before surgery through a standard

264 blood draw protocol. Fresh frozen tumor tissue was collected from surgery. Tumor tissues,  
265 matched white blood cells (WBC) and PLF pellets were stored at -80°C until DNA extraction. In  
266 total, PLF, frozen tumor tissue and blood samples were collected for analysis from 104  
267 patients.

268

### 269 **Cell lines and standard reference**

270 The two cancer cell lines hepatocarcinoma PLC/PRF/5 cells and lung carcinoma A549 cells  
271 used to construct the cancer cell fraction model were both obtained from the Cell Bank of the  
272 Chinese Academy of Sciences (Shanghai, China). In the model, PLC cells were used as the  
273 “tumor cells” and diluted with A549 cells which were used as the “normal cells”. The two cell  
274 lines were counted with FACS Aria SORP flow cytometry (Becton Dickinson; San Diego,  
275 CA, USA) and serially diluted for a total of 9 dilutions (PLC cell fraction = 0%, 0.0001%,  
276 0.0003%, 0.001%, 0.005%, 0.05%, 0.5%, 5% and 33%). The details of the model construction  
277 and number of cells are shown in Supplementary Table 4.

278

### 279 **DNA extraction and library preparation**

280 Genomic DNAs were extracted from PLF, frozen tumor tissue, WBC and cell line samples  
281 using the QIAamp DNA Mini Kit (Qiagen; Hilden, Germany). Exome sequencing was  
282 performed on genomic DNA (1000 ng) from frozen tumor tissue and WBC, and customized  
283 panel targeting 20 mutations was performed on genomic DNA (200 ng) from cell lines or PLF.  
284 Genomic DNA was sheared into small fragments (mean length ~ 200 bp) with the Covaris  
285 E220 instrument (Covaris; Woburn, MA, USA). The sheared DNA was prepared for genomic

286 libraries using the KAPA Hyper Prep Kit (Roche; Basel, Switzerland) through a series of  
287 enzymatic steps including, end-repair, dA tailing, ligation of adaptors and amplification  
288 following standard protocols except that for the use of a customized adaptor with barcodes for  
289 PLF and cell line samples as previously described<sup>32,49</sup>.

290

### 291 **Whole-exome sequencing and identification of somatic mutations**

292 Whole genome libraries of tumor and matched WBC DNAs were enriched for exome regions  
293 with Agilent SureSelectXT Human All Exon V5 probe and reagents (Agilent; Santa Clara, CA,  
294 USA). The captured and amplified libraries were sequenced on the Illumina HiSeqX Ten with  
295 150-bp paired-end sequencing to a median depth of 183× for tumor tissue samples and 105×  
296 for WBC samples after removing duplicate molecules. The sequencing raw data (FASTQ file)  
297 were aligned to the UCSC human reference genome hg19 using the Burrows-Wheeler aligner  
298 software (BWA, v0.7.15). Basic processing, marking duplicates, local realignments and score  
299 recalibration were analyzed using The Genome Analysis Toolkit (GATK, v3.6), Picard (v2.7.1)  
300 and Samtools (v1.3.1). Candidate somatic mutations were detected by comparing sequencing  
301 data from tumor tissue samples with MuTect1 and Strelka. All selected mutations were further  
302 validated with manual inspection using Integrated Genome Viewer (IGV)<sup>50</sup>.

303

### 304 **Targeted sequencing in cell line samples**

305 The whole genome libraries generated from cell line DNA were captured using a 63-gene  
306 panel (Supplementary Table 8, 202 kb) and Agilent SureSelect hybrid capture reagents. The  
307 sequencing and analysis flow of the captured library is consistent with that of whole exome

308 sequencing (WES). PLC cells were used as the tumor sample and A549 cells were used as  
309 the normal cell sample, with a median depth of 8221× distinct high quality reads for PLC  
310 samples and 6721× for A549 samples. 20 SNPs specific for PLC were chosen and compared  
311 with A459. These SNPs were assessed in the diluted cell line samples where the mutation  
312 frequency was 100% in the PLC cell line and 0% in the A549 cell line using the previously  
313 described method<sup>32</sup>. Experiments were repeated three times on samples from each dilution  
314 and 20 times for the 0% PLC cell fraction. Targeted sequencing achieved median  
315 pre-deduplication sequencing depths of 415,165× and 20,074× after removing duplicate  
316 molecules for each detection SNP.

317

#### 318 **Customized assay to profile multiple mutations**

319 Genomic DNAs (200 ng) from cell lines or PLF were used for the customized panel targeting  
320 20 mutations. The ligation products with customized adaptor were amplified for a whole  
321 genome library and used as template to profile mutations identified in the matched tumor  
322 tissue. The customized adaptor contained sufficient unique DNA barcodes identifying each  
323 original molecule<sup>32</sup>. We selected 20 tumor-specific somatic mutations from the WES results of  
324 tumor tissue for primer design. For each patient, the 20 tumor-specific variants were selected  
325 according to the potential to be a driver mutation (Supplementary Table 9), the confidence of  
326 the mutation by IGV and the frequency of the mutation. Oligo software (v7.53) was used to  
327 design multiplex-PCR primer pairs for the two rounds of nested amplification and verified  
328 uniqueness in the human genome (<http://genome.ucsc.edu/>) to ensure amplification efficiency.  
329 In the first round of amplification, the target regions were amplified in 9 cycles of PCR using a

330 target-specific primer and a primer matching the adapter sequence. A second round of 14  
331 cycles of amplification was performed with one pair of nested primers matching the adapter  
332 and the target region to further enrich the target region and add the Illumina adapter  
333 sequences to the construct. This method can amplify more than 200 target regions in parallel.  
334 The targeted sequencing libraries were sequenced on the Illumina Novaseq 6000 with a  
335 median depth of 101,703× before de-duplication and 11,760× after removing duplicate  
336 molecules. The on-target ratio of reads mapped to the target region was 80% in median.

337

### 338 **Bioinformatics pipeline and SNV calling**

339 With the DNA barcode in the customized adapter, redundant reads can be tracked from an  
340 original DNA molecule to minimize false positive calling due to PCR amplification and  
341 sequencing errors. Sequencing reads were mapped to the hg19 reference genome using 'bwa  
342 mem' with the default parameters after extracting tags and removing sequence adapters. The  
343 SNV analysis mutation frequency calculation method was used as previously described<sup>32</sup>.  
344 Briefly, reads with the same tags and start and end coordinates were grouped into Unique  
345 Identifier families (UID families). If > 80% of the reads in a UID family harbor the same  
346 mutation identified in the matched tumor tissue, the UID family was defined as an Effective  
347 Unique Identifier family (EUID family) with the mutation. The mutant EUID families were further  
348 confirmed by manual inspection (IGV) and used to calculate the frequency of the mutation with  
349 the total number of UID families covering the mutant site.

350

### 351 **PLF mutation profiling model**

352 Estimated cancer cell fraction analysis was performed in the R statistical environment version  
353 3.6.3.

354 Assumption: 1. Because of the low fraction of residual cancer cells among normal cells in  
355 PLF, there are chances that some mutations present in the tumor tissue are not detected in the  
356 corresponding PLF sample. The algorithm is also based on the assumption that this  
357 tumor-PLF mismatch results from the low concentration of mutant molecules and/or the  
358 randomness in sampling. 2. The estimation model is based on the assumption that mutant  
359 allele reads and non-mutant wild-type allele reads fit well with the binomial distribution.

360 Let  $(m_1, m_2, \dots, m_{n-1}, m_n)$  be N mutations in PLF, each with a mutation frequency of  $P_{C_i}$ ,  
361 sequencing depth of  $D_i$ , mutation reads number of  $A_i$ . And  $P_{t_i}$  indicates the mutation  
362 frequency in the corresponding solid tumor tissue. If R is the overall cancer cell concentration  
363 of this sample, then for mutation  $m_i$ , the mutational frequency in PLF,  $P_{C_i} = P_{t_i} * R$ , and the  
364 distribution of observing  $X_i$  reads with mutation  $m_i$  out of  $D_i$  reads in PLF follow the  
365 binomial distribution:

$$X_i \sim B(D_i, P_{C_i})$$

366 Then the probability of observing  $A_i$  reads with mutation  $m_i$  out of  $D_i$  reads at position  $m_i$   
367 is:

$$P_i(X_i = A_i) = \binom{D_i}{A_i} P_{C_i}^{A_i} (1 - P_{C_i})^{D_i - A_i}$$

368 Assuming that the events of observing  $(A_1, A_2, \dots, A_{n-1}, A_n)$  reads supports that mutations  
369  $(m_1, m_2, \dots, m_{n-1}, m_n)$  are independent, then the probability of observing a sequence of  
370  $(A_1, A_2, \dots, A_{n-1}, A_n)$  is the product of  $P_i(X_i = A_i)$  for each mutation  $m_i$ . Let  $P$  be the  
371 likelihood function of cancer cell concentration  $R$ :

$$L(R) = P = \prod_{i=1}^n P_i = \prod_{i=1}^n \binom{D_i}{A_i} (Pt_i * R)^{A_i} (1 - Pt_i * R)^{D_i - A_i}$$

372 And  $P$  is maximized to obtain the predicted  $R$ , namely  $\hat{R}$ :

$$\begin{aligned} \hat{R} &= \arg \max_R \prod_{i=1}^n P_i = \prod_{i=1}^n \binom{D_i}{A_i} (Pt_i * R)^{A_i} (1 - Pt_i * R)^{D_i - A_i} \\ &= \arg \max_R \ln \left[ \prod_{i=1}^n \binom{D_i}{A_i} (Pt_i * R)^{A_i} (1 - Pt_i * R)^{D_i - A_i} \right] \end{aligned}$$

373

$$= \arg \max_R \sum_{i=1}^n \left[ \ln \binom{D_i}{A_i} + A_i * \ln(Pt_i * R) + (D_i - A_i) * \ln(1 - Pt_i * R) \right]$$

374 A search through a grid (0.00001, 1, step=0.00001) for  $R$  in the above formula yields the  
375 optimized  $\hat{R}$ . Maximum mutation frequencies in tumor tissues were used for normalization of  
376 tumor sample purity.

377

### 378 **Statistics**

379 Recurrence-free survival (RFS) was calculated as the time from surgery to the date of  
380 recurrence, last visit or death, whichever comes first. Overall survival (OS) was measured from  
381 surgery to the date of cause-specific death or last visit. Survival curves were plotted and  
382 analyzed with the Kaplan–Meier method, and the log-rank test was used to test the  
383 significance of the difference between survival curves.

384 In addition to the cancer cell fraction, the prognostic impact of other factors, such as  
385 Lauren classification, pathology T/N stage, cytology, lymphovascular and nerve invasion were  
386 also analyzed. HRs were first estimated using univariate Cox proportional hazard models.

387 Thereafter, factors with statistical significance ( $p < 0.05$ ) were further assessed in multivariate

388 analysis using the Cox proportional hazard model. Whenever there was no event in one group  
389 of categorical variables, Firth's penalized likelihood was adopted to allow for monotone  
390 likelihood (R package "coxphf"). All statistical analysis was performed using the survival  
391 package or coxphf package from the R software (V.3.6.3). Statistical comparison of the cancer  
392 cell fraction distribution in patients with no recurrence, peritoneal dissemination or lymphatic  
393 metastasis was performed using 2-tailed Wilcoxon Mann-Whitney U test with significance level  
394 set at 5% and results are expressed as mean  $\pm$  SD.  $P < 0.05$  was considered statistically  
395 significant.

396

#### 397 **Data availability**

398 The sequencing data from tumor tissue, WBC and PLF samples have been deposited at the  
399 Genome Sequence Archive for Human under the accession code HRA000528  
400 (<https://bigd.big.ac.cn/gsa-human/>).

401

#### 402 **Study approval**

403 All patients provided written informed consent, and the study was approved by Ethics  
404 Committee of National Cancer Center, Cancer Hospital, Chinese Academy of Medical  
405 Sciences and Peking Union Medical College (approval number: 17-093/1349).

406

407 **Author Contributions**

408 D.Z.: designed the study, organized sample collection, acquired data, interpreted data, and  
409 provided study supervision. P.Y.: performed experiments, analysed data, interpreted data, and  
410 wrote the manuscript. T.W.: Organized patient enrollment, sample collection, and clinical data  
411 curation. P.W.: developed and optimized experimental protocols, and analysed data. Q.S.:  
412 analyzed data. J.W.: interpreted data and wrote the manuscript. Y.J.: designed the study,  
413 acquired, analyzed and interpreted data, wrote the manuscript, and provided study supervision.  
414 All authors critically reviewed the manuscript.

415

416 **Acknowledgments:** This study was supported by National Key R&D Program of China  
417 (2018YFC1312100), the Chinese Academy of Medical Sciences (CAMS) Innovation Fund for  
418 Medical Sciences (CIFMS) (2016-I2M-1-001, 2019-I2M-1-003 and 2017-I2M-4-002).

419

420 **Correspondence** and requests for materials should be addressed to Yuchen Jiao.

421 **Conflict of interest:** Y.J. is one of the cofounders and have owner interest in Genetron  
422 Holdings, and receives royalties from Genetron. Y.J., D.Z., P.W., Q.S., and P.Y. have filed  
423 patents/patent applications based on the technology and data generated from this work. The  
424 remaining authors disclose no conflicts.

425

426 **REFERENCES**

- 427 1 Bray, F. et al. Global cancer statistics 2018: GLOBOCAN estimates of incidence and mortality  
428 worldwide for 36 cancers in 185 countries. *CA Cancer J Clin* **68**, 394-424 (2018).
- 429 2 Badgwell, B. et al. Long-term survival in patients with metastatic gastric and gastroesophageal  
430 cancer treated with surgery. *J Surg Oncol* **111**, 875-881 (2015).
- 431 3 Kuramoto, M. et al. Extensive intraoperative peritoneal lavage as a standard prophylactic strategy  
432 for peritoneal recurrence in patients with gastric carcinoma. *Ann Surg* **250**, 242-246 (2009).
- 433 4 Desiderio, J. et al. The 30-year experience-A meta-analysis of randomised and high-quality  
434 non-randomised studies of hyperthermic intraperitoneal chemotherapy in the treatment of gastric  
435 cancer. *Eur J Cancer* **79**, 1-14 (2017).
- 436 5 Yonemura, Y. et al. Intraoperative chemohyperthermic peritoneal perfusion as an adjuvant to  
437 gastric cancer: final results of a randomized controlled study. *Hepatogastroenterology* **48**,  
438 1776-1782 (2001).
- 439 6 Kim, J. Y. & Bae, H. S. A controlled clinical study of serosa-invasive gastric carcinoma patients who  
440 underwent surgery plus intraperitoneal hyperthermo-chemo-perfusion (IHCP). *Gastric Cancer* **4**,  
441 27-33 (2001).
- 442 7 Roviello, F., Caruso, S., Neri, A. & Marrelli, D. Treatment and prevention of peritoneal  
443 carcinomatosis from gastric cancer by cytoreductive surgery and hyperthermic intraperitoneal  
444 chemotherapy: overview and rationale. *Eur J Surg Oncol* **39**, 1309-1316 (2013).
- 445 8 Gill, R. S. et al. Treatment of gastric cancer with peritoneal carcinomatosis by cytoreductive surgery  
446 and HIPEC: a systematic review of survival, mortality, and morbidity. *J Surg Oncol* **104**, 692-698  
447 (2011).
- 448 9 Mizrak Kaya, D. et al. Risk of peritoneal metastases in patients who had negative peritoneal staging  
449 and received therapy for localized gastric adenocarcinoma. *J Surg Oncol* **117**, 678-684 (2018).
- 450 10 Chen, Y. et al. Predicting Peritoneal Dissemination of Gastric Cancer in the Era of Precision  
451 Medicine: Molecular Characterization and Biomarkers. *Cancers (Basel)* **12** (2020).
- 452 11 Yang, X. J., Li, Y. & Yonemura, Y. Cytoreductive surgery plus hyperthermic intraperitoneal  
453 chemotherapy to treat gastric cancer with ascites and/or peritoneal carcinomatosis: Results from a  
454 Chinese center. *J Surg Oncol* **101**, 457-464 (2010).
- 455 12 Lisiecki, R., Kruszwicka, M., Sychala, A. & Murawa, D. Prognostic significance, diagnosis and  
456 treatment in patients with gastric cancer and positive peritoneal washings. A review of the  
457 literature. *Rep Pract Oncol Radiother* **22**, 434-440 (2017).
- 458 13 Wang, J.-Y. et al. Gastric cancer cell detection in peritoneal lavage: RT-PCR for carcinoembryonic  
459 antigen transcripts versus the combined cytology with peritoneal carcinoembryonic antigen levels.  
460 *Cancer Letters* **223**, 129-135 (2005).
- 461 14 Yonemura, Y. et al. Inhibition of peritoneal dissemination in human gastric cancer by  
462 MMP-7-specific antisense oligonucleotide. *J Exp Clin Cancer Res* **20**, 205-212 (2001).
- 463 15 Tokuda, K. et al. Clinical significance of CEA-mRNA expression in peritoneal lavage fluid from  
464 patients with gastric cancer. *Int J Mol Med* **11**, 79-84 (2003).
- 465 16 Kodera, Y. et al. Prognostic significance of intraperitoneal cancer cells in gastric carcinoma: analysis  
466 of real time reverse transcriptase-polymerase chain reaction after 5 years of followup. *J Am Coll*  
467 *Surg* **202**, 231-236 (2006).
- 468 17 Nakanishi, H. et al. Rapid quantitative detection of carcinoembryonic antigen-expressing free

469 tumor cells in the peritoneal cavity of gastric-cancer patients with real-time RT-PCR on the  
470 lightcycler. *Int J Cancer* **89**, 411-417 (2000).

471 18 Kodera, Y. et al. Quantitative detection of disseminated free cancer cells in peritoneal washes with  
472 real-time reverse transcriptase-polymerase chain reaction: a sensitive predictor of outcome for  
473 patients with gastric carcinoma. *Ann Surg* **235**, 499-506 (2002).

474 19 Kodera, Y. et al. Prognostic significance of intraperitoneal cancer cells in gastric carcinoma:  
475 detection of cytokeratin 20 mRNA in peritoneal washes, in addition to detection of  
476 carcinoembryonic antigen. *Gastric Cancer* **8**, 142-148 (2005).

477 20 Yonemura, Y. et al. Prediction of peritoneal micrometastasis by peritoneal lavaged cytology and  
478 reverse transcriptase-polymerase chain reaction for matrix metalloproteinase-7 mRNA. *Clin Cancer*  
479 *Res* **7**, 1647-1653 (2001).

480 21 Kim, Y. J. et al. The Detection of Messenger RNA for Carcinoembryonic Antigen and Cytokeratin 20  
481 in Peritoneal Washing Fluid in Patients with Advanced Gastric Cancer. *Korean J Gastroenterol* **69**,  
482 220-225 (2017).

483 22 Tokuhisa, M. et al. Exosomal miRNAs from Peritoneum Lavage Fluid as Potential Prognostic  
484 Biomarkers of Peritoneal Metastasis in Gastric Cancer. *PLoS One* **10**, e0130472 (2015).

485 23 Ohzawa, H. et al. Reduced expression of exosomal miR-29s in peritoneal fluid is a useful predictor  
486 of peritoneal recurrence after curative resection of gastric cancer with serosal involvement. *Oncol*  
487 *Rep* **43**, 1081-1088 (2020).

488 24 Hiraki, M. et al. Aberrant gene methylation is a biomarker for the detection of cancer cells in  
489 peritoneal wash samples from advanced gastric cancer patients. *Ann Surg Oncol* **18**, 3013-3019  
490 (2011).

491 25 Ushiku, H. et al. DNA diagnosis of peritoneal fluid cytology test by CDO1 promoter DNA  
492 hypermethylation in gastric cancer. *Gastric Cancer* **20**, 784-792 (2017).

493 26 McDonald, B. R. et al. Personalized circulating tumor DNA analysis to detect residual disease after  
494 neoadjuvant therapy in breast cancer. *Sci Transl Med* **11** (2019).

495 27 Leal, A. et al. White blood cell and cell-free DNA analyses for detection of residual disease in  
496 gastric cancer. *Nat Commun* **11**, 525 (2020).

497 28 Abbosh, C. et al. Phylogenetic ctDNA analysis depicts early-stage lung cancer evolution. *Nature* **545**,  
498 446-451 (2017).

499 29 Azad, T. D. et al. Circulating Tumor DNA Analysis for Detection of Minimal Residual Disease After  
500 Chemoradiotherapy for Localized Esophageal Cancer. *Gastroenterology* **158**, 494-505.e496 (2020).

501 30 Reinert, T. et al. Analysis of Plasma Cell-Free DNA by Ultradeep Sequencing in Patients With Stages  
502 I to III Colorectal Cancer. *JAMA Oncol* **5**, 1124-1131 (2019).

503 31 Christensen, E. et al. Early Detection of Metastatic Relapse and Monitoring of Therapeutic Efficacy  
504 by Ultra-Deep Sequencing of Plasma Cell-Free DNA in Patients With Urothelial Bladder Carcinoma.  
505 *J Clin Oncol* **37**, 1547-1557 (2019).

506 32 Qu, C. et al. Detection of early-stage hepatocellular carcinoma in asymptomatic  
507 HBsAg-seropositive individuals by liquid biopsy. *Proc Natl Acad Sci U S A* **116**, 6308-6312 (2019).

508 33 Patel, J. P. et al. Prognostic relevance of integrated genetic profiling in acute myeloid leukemia. *N*  
509 *Engl J Med* **366**, 1079-1089 (2012).

510 34 Schuurhuis, G. J. et al. Minimal/measurable residual disease in AML: a consensus document from  
511 the European LeukemiaNet MRD Working Party. *Blood* **131**, 1275-1291 (2018).

512 35 Thomassen, I. et al. Peritoneal carcinomatosis of gastric origin: a population-based study on

513 incidence, survival and risk factors. *Int J Cancer* **134**, 622-628 (2014).

514 36 Jung, Y. J., Seo, H. S., Kim, J. H., Park, C. H. & Lee, H. H. Cross-Sectional Location of Gastric Cancer  
515 Affects the Long-Term Survival of Patients as Tumor Invasion Deepens. *Ann Surg Oncol* **24**,  
516 3947-3953 (2017).

517 37 La Torre, M. et al. Peritoneal wash cytology in gastric carcinoma. Prognostic significance and  
518 therapeutic consequences. *Eur J Surg Oncol* **36**, 982-986 (2010).

519 38 Coccolini, F. et al. Peritoneal carcinomatosis. *World J Gastroenterol* **19**, 6979-6994 (2013).

520 39 Katsuragi, K. et al. Prognostic impact of PCR-based identification of isolated tumour cells in the  
521 peritoneal lavage fluid of gastric cancer patients who underwent a curative R0 resection. *Br J*  
522 *Cancer* **97**, 550-556 (2007).

523 40 Bentrem, D., Wilton, A., Mazumdar, M., Brennan, M. & Coit, D. The value of peritoneal cytology as  
524 a preoperative predictor in patients with gastric carcinoma undergoing a curative resection. *Ann*  
525 *Surg Oncol* **12**, 347-353 (2005).

526 41 Hiraki, M. et al. Aberrant gene methylation in the peritoneal fluid is a risk factor predicting  
527 peritoneal recurrence in gastric cancer. *World J Gastroenterol* **16**, 330-338 (2010).

528 42 Yonemura, Y. et al. Diagnostic value of preoperative RT-PCR-based screening method to detect  
529 carcinoembryonic antigen-expressing free cancer cells in the peritoneal cavity from patients with  
530 gastric cancer. *ANZ J Surg* **71**, 521-528 (2001).

531 43 Coombes, R. C. et al. Personalized Detection of Circulating Tumor DNA Antedates Breast Cancer  
532 Metastatic Recurrence. *Clin Cancer Res* **25**, 4255-4263 (2019).

533 44 Dudley, J. C. et al. Detection and Surveillance of Bladder Cancer Using Urine Tumor DNA. *Cancer*  
534 *Discov* **9**, 500-509 (2019).

535 45 Razavi, P. et al. High-intensity sequencing reveals the sources of plasma circulating cell-free DNA  
536 variants. *Nat Med* **25**, 1928-1937 (2019).

537 46 Li, J. K. et al. Peritoneal lavage cytology and carcinoembryonic antigen determination in predicting  
538 peritoneal metastasis and prognosis of gastric cancer. *World J Gastroenterol* **11**, 7374-7377 (2005).

539 47 Oyama, K., Terashima, M., Takagane, A. & Maesawa, C. Prognostic significance of peritoneal  
540 minimal residual disease in gastric cancer detected by reverse transcription-polymerase chain  
541 reaction. *Br J Surg* **91**, 435-443 (2004).

542 48 Leake, P. A. et al. A systematic review of the accuracy and utility of peritoneal cytology in patients  
543 with gastric cancer. *Gastric Cancer* **15 Suppl 1**, S27-37 (2012).

544 49 Zhang, W. et al. Genetic Features of Aflatoxin-Associated Hepatocellular Carcinoma.  
545 *Gastroenterology* **153**, 249-262.e242 (2017).

546 50 Fujikura, K. et al. Multiregion whole-exome sequencing of intraductal papillary mucinous  
547 neoplasms reveals frequent somatic KLF4 mutations predominantly in low-grade regions. *Gut*  
548 (2020).

549

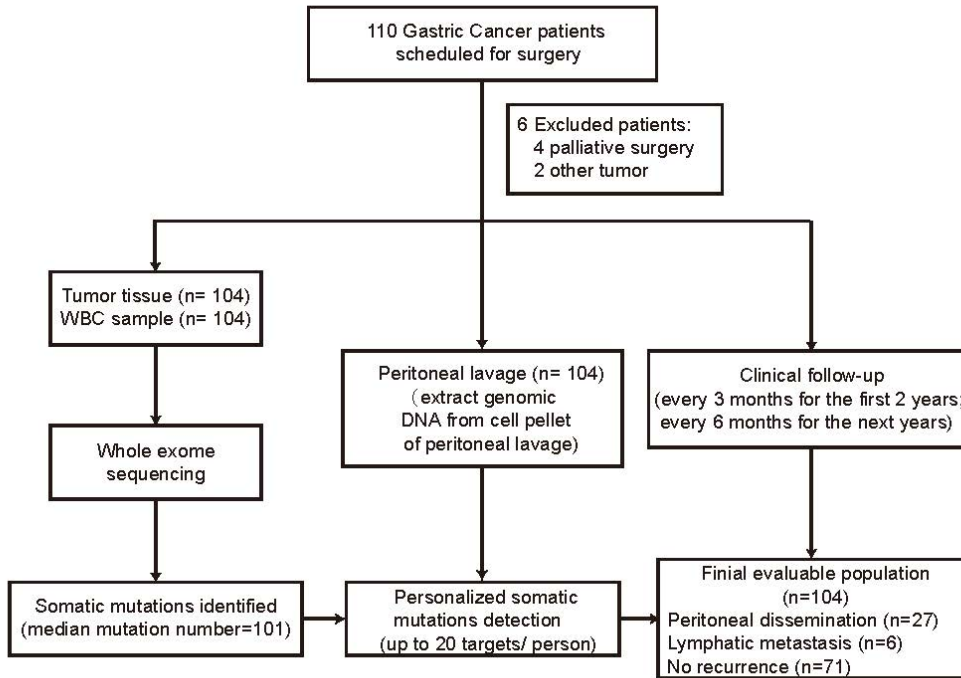
550

551

552

553 **Fig. 1 Patient enrollment, sample detection workflow and the prognosis prediction of**  
554 **patients.**

555 Fig. 1 Patient enrollment, sample detection workflow and the prognosis prediction of patients.



564

565

566

567

568

569

570

571

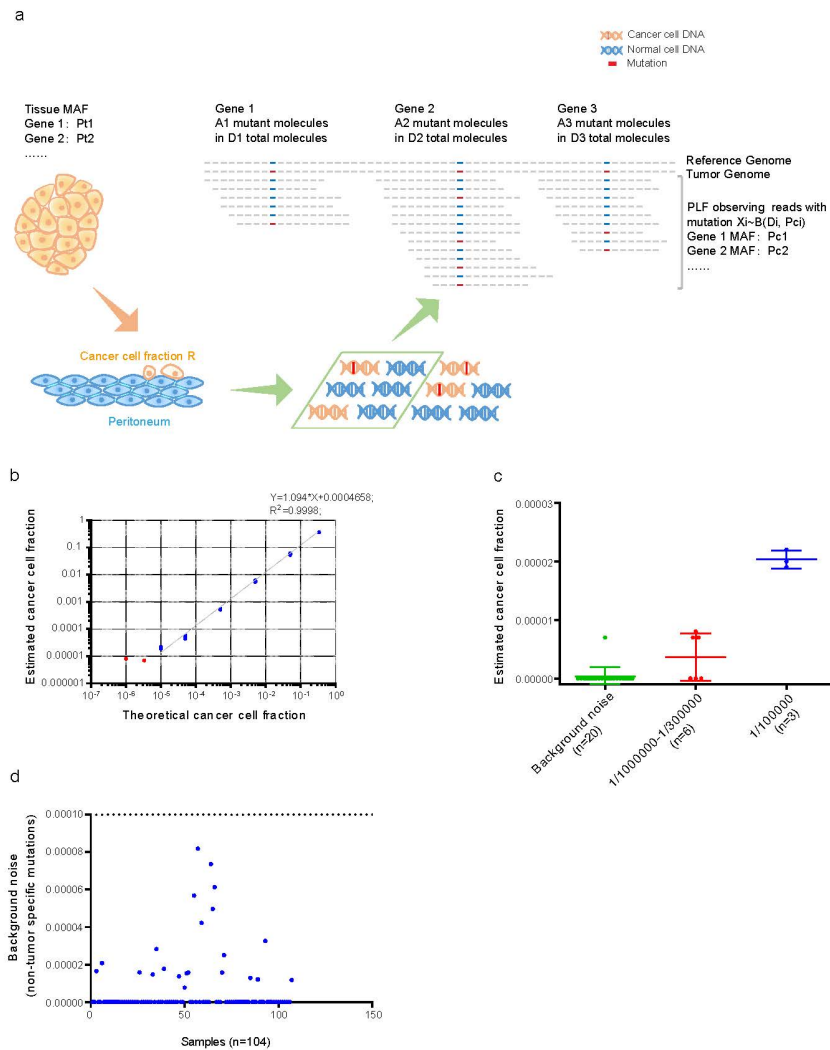
572

573

574

575 **Fig. 2 Cancer cell fraction model and background noise.**

576 Fig. 2 Cancer cell fraction model and background noise.



590 (a). Cancer cell fraction model. A model to estimate the cancer cell fraction based on allele  
 591 frequency and sequencing depth of somatic mutations in tumor tissue and paired PLF samples.  
 592 MAF: mutant allele frequency;  $P_{t_i}$ : MAF in solid tumor tissue;  $P_{c_i}$ : MAF in corresponding  
 593 peritoneal lavage fluid (PLF);  $D_i$ : sequencing depth in PLF;  $A_i$ : mutation reads number in PLF;  
 594  $X_i$ : observing reads with mutation in PLF; and R: overall cancer cell concentration.

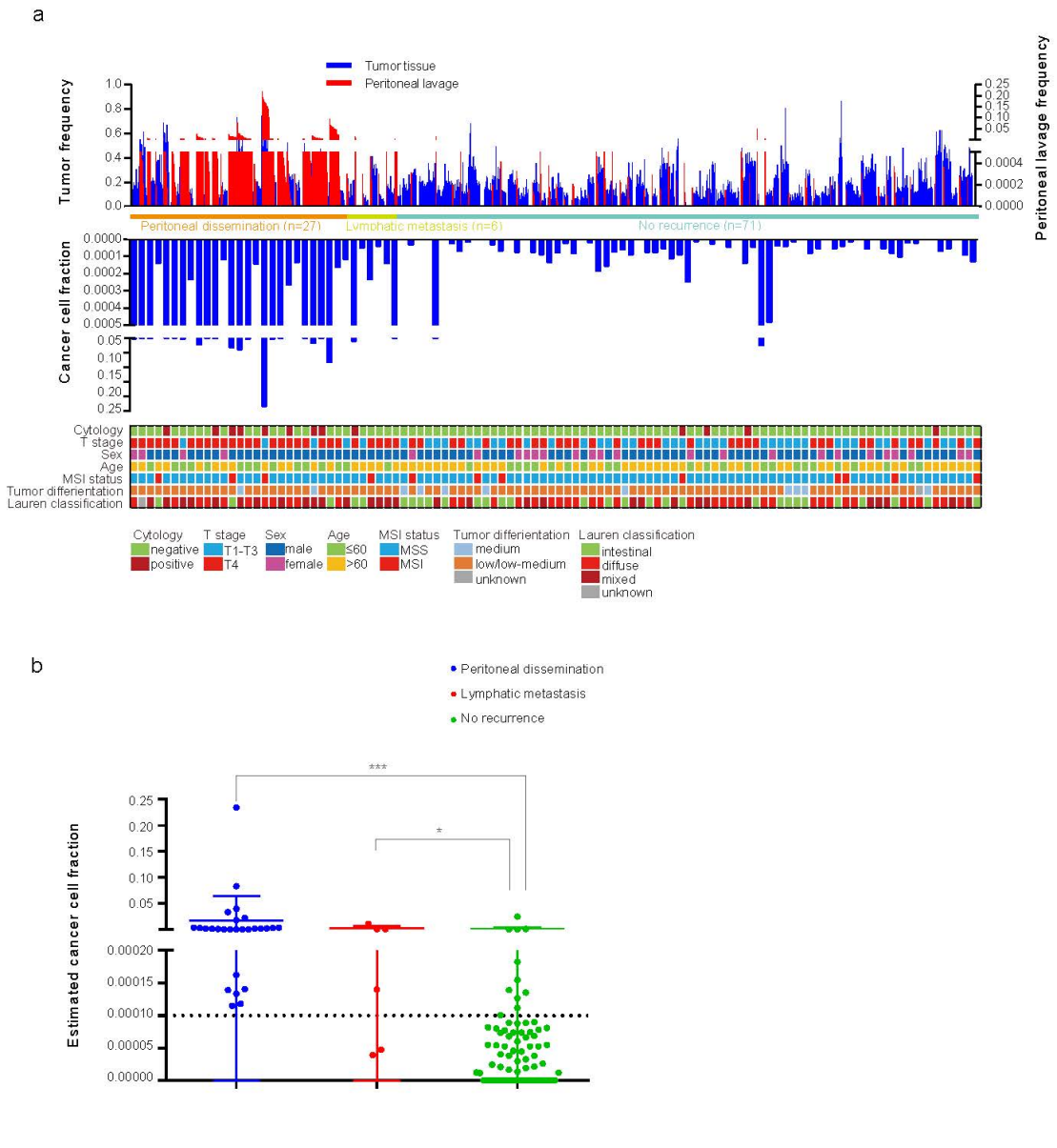
595 (b). The linear correlation between theoretical and estimated cancer cell fraction up to the  
 596 dilution of  $1:10^{-5}$ . Each dilution was repeated three times. The blue dots highlight the fractions  
 597 above the limit of detection (PLC/PRF/5 cell fraction = 0.001%, 0.005%, 0.05%, 0.5%, 5% and  
 598 33%). The red dots highlight the fractions under the limit of detection (PLC/PRF/5 cell fraction  
 599 = 0.0001%, 0.0003%).

600 (c). Background noise observed in the cancer cell fraction model at 0% PLC/PRF/5 cell input  
 601 among the 20 independent replicates (green dots). Experiments performed on different cell  
 602 line dilutions (0.0001% and 0.0003%, red dots; 0.001%, blue dots) were repeated three times.

603 (d). Biological noise of the 104 PLF samples from patients. The cancer cell fraction for each  
 604 sample was calculated based on non-tumor-specific mutations.

**Fig. 3 Summary of clinical and histopathologic parameters, somatic mutations and cancer cell fraction for all patients.**

Fig. 3 Summary of clinical and histopathologic parameters, somatic mutations and cancer cell fraction for all patients.



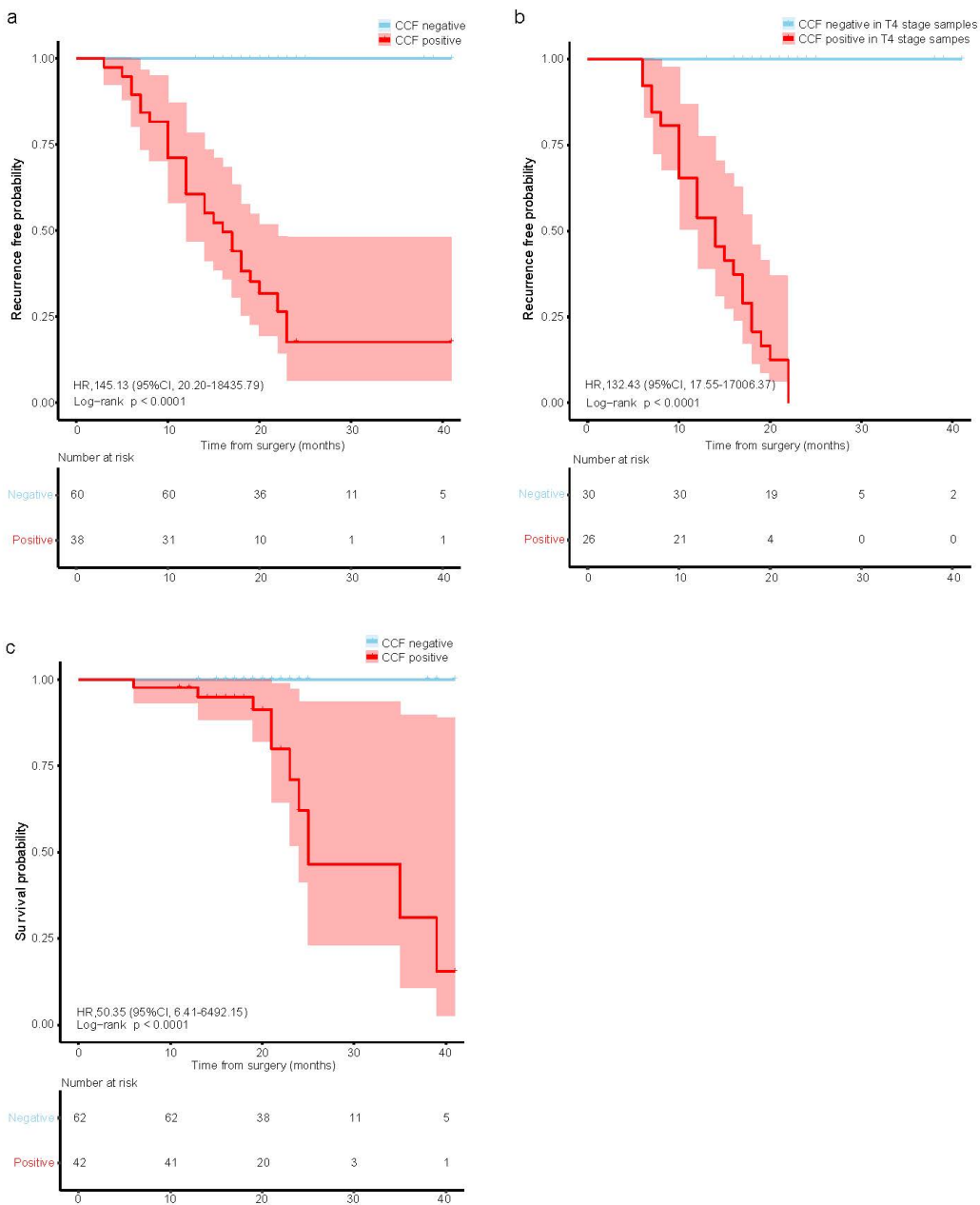
(a). Top panel, the summary of the frequencies of the tracked mutations in tumor and matched peritoneal lavage fluid samples from 104 patients. Blue bar, the tumor frequency of each tracked mutation. Frequency values are shown on the left vertical axis. Red bar, the detected peritoneal lavage fluid frequency of each tracked mutation. Frequency values are shown on the right vertical axis. The clinical outcome of patients is indicated under the bar. Middle panel, the summary of the cancer cell fractions for each patient. Bottom panel, clinical and histopathologic characteristics.

(b). The cancer cell fraction distribution in patients with peritoneal dissemination ( $n = 27$ ), lymphatic metastasis ( $n = 6$ ) or no recurrence ( $n = 71$ ). Reported p values are computed using 2-tailed Wilcoxon Mann-Whitney U test.

\*\*\*,  $p < 0.001$ ; \*,  $p < 0.05$

649 **Fig. 4 Kaplan-Meier estimates of recurrence-free survival (RFS) and overall survival (OS)**  
 650 **for gastric cancer patients.**

651 Fig. 4 Kaplan-Meier estimates of recurrence-free survival (RFS) and overall survival (OS) for gastric cancer patients.



684 (a) and (b). Kaplan-Meier survival analysis shows probability of recurrence-free survival (RFS)  
 685 as determined by A. cancer cell fraction detected in peritoneal lavage fluid ( $n = 98$ ); and B.  
 686 cancer cell fraction detected in peritoneal lavage fluid in stage T4 patients ( $n = 56$ ) (for  
 687 peritoneal dissemination). A patient was classified as testing positive if the cancer cell fraction  
 688 detected in peritoneal lavage fluid was  $\geq 0.01\%$ ;

689 (c) Kaplan-Meier estimates of overall survival (OS) for 104 gastric cancer patients based on  
 690 the estimated cancer cell fraction in peritoneal lavage fluid.

691 Shaded areas in the Kaplan-Meier plots indicate 95%CI. HR: hazard ratio; CCF: cancer cell  
 692 fraction.

**Table 1 Binary results of the PLF mutation profiling model and clinical risk factors**

		Estimated cancer cell fraction		Cytological diagnosis		Pathologic diagnosis	
Risk of		true PD	true noPD	true PD	true noPD	true PD	true noPD
peritoneal	predict PD	27	11	8	4	23	33
dissemination	predict noPD	0	60	19	67	4	38
(n = 98)	Sensitivity	100%		30%		85%	
	Specificity		85%		94%		54%
	PPV	71%		67%		41%	
	NPV		100%		78%		90%
Risk of		true RE	true noRE	true RE	true noRE	true RE	true noRE
recurrence	predict RE	31	11	9	4	28	33
(n = 104)	predict noRE	2	60	24	67	5	38
	Sensitivity	94%		27%		85%	
	Specificity		85%		94%		54%
	PPV	74%		69%		46%	
	NPV		97%		74%		88%

PD, peritoneal dissemination; RE, recurrence; PPV, positive predictive value; NPV, negative predictive value.

Estimated cancer cell fraction was defined as positive (CCF  $\geq$  0.01%) or negative (CCF  $<$  0.01%).

Pathologic diagnosis was defined as high (T4) or low (T0-3) according to the standard criteria.

# Figures

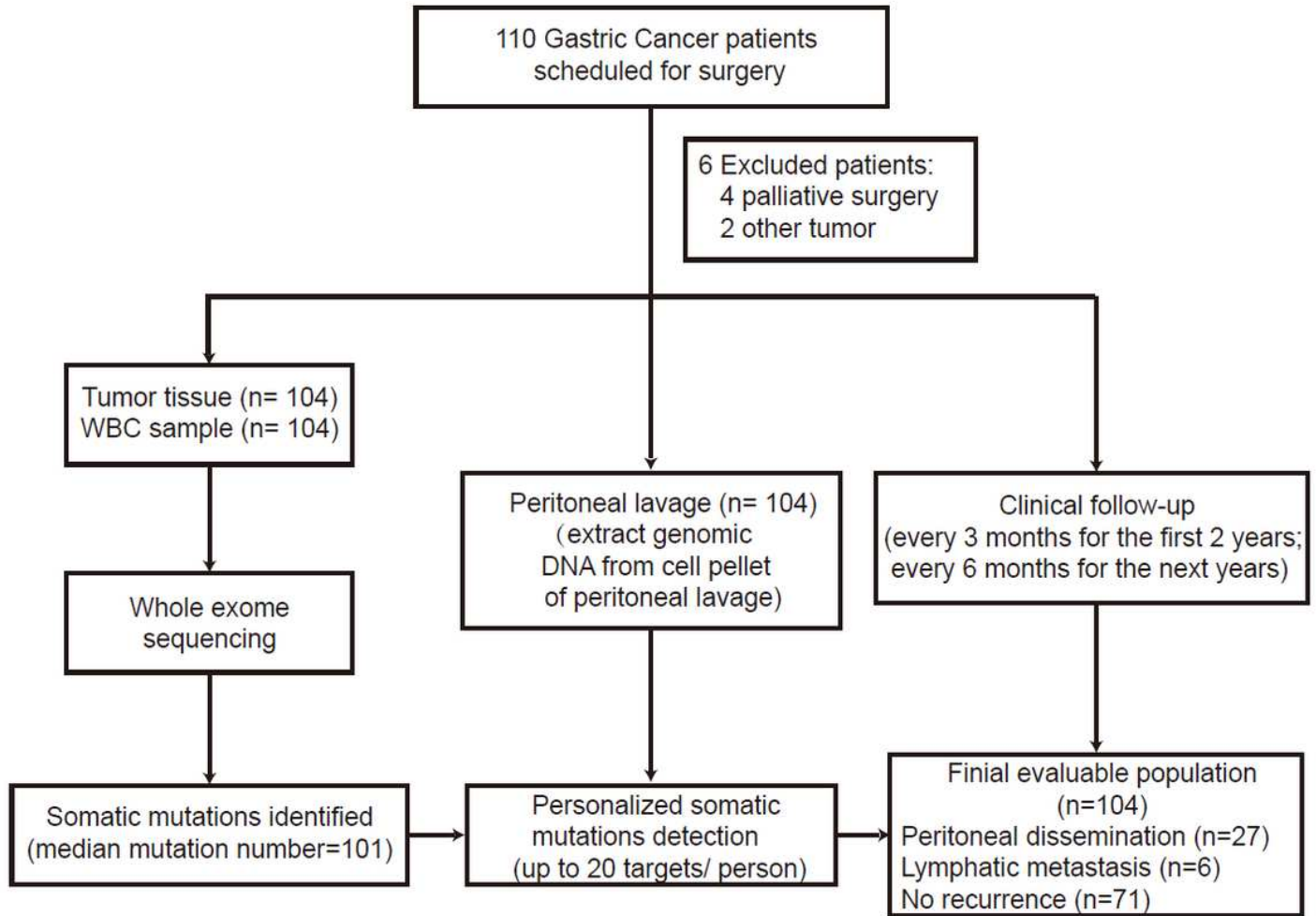
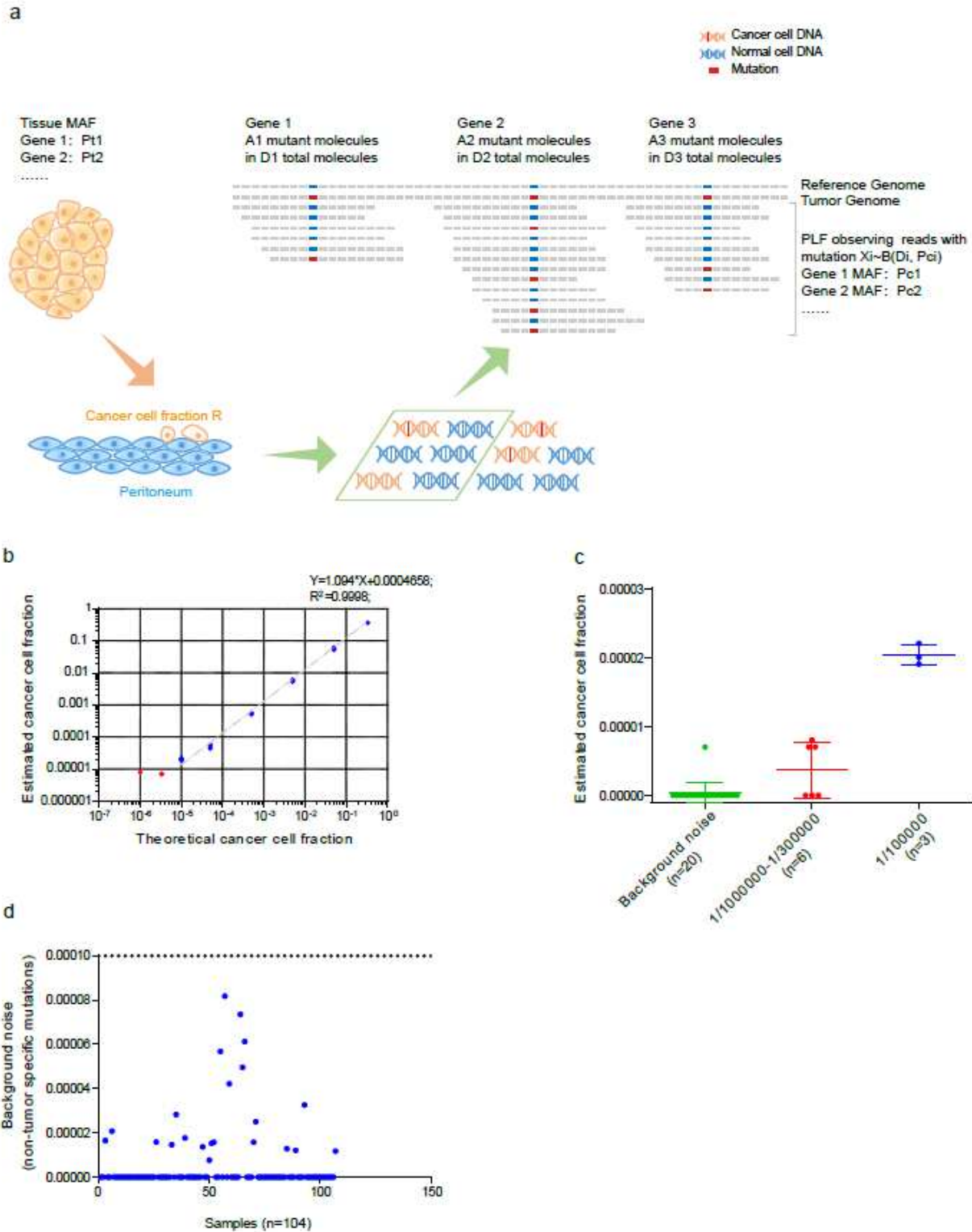


Figure 1

Patient enrollment, sample detection workflow and the prognosis prediction of patients.

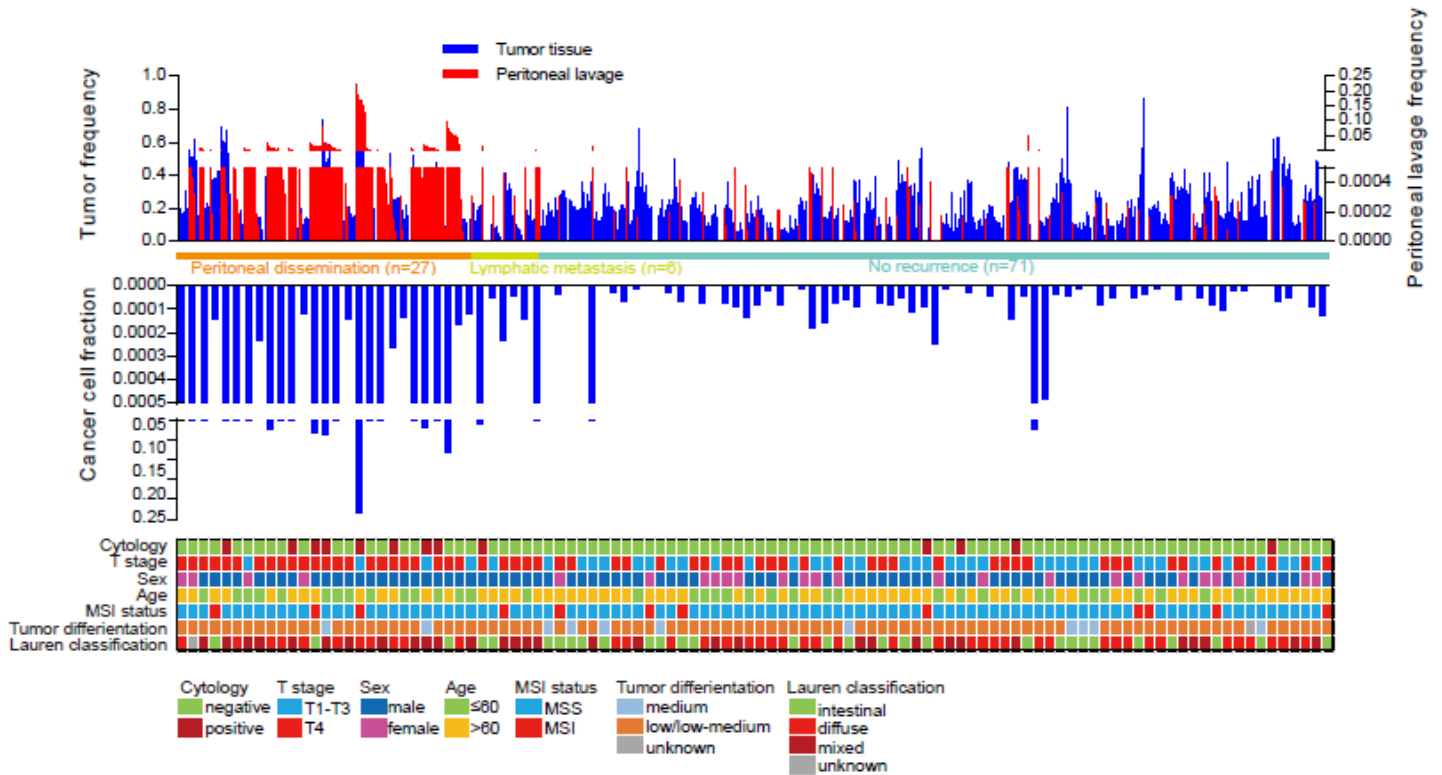


**Figure 2**

Cancer cell fraction model and background noise. (a). Cancer cell fraction model. A model to estimate the cancer cell fraction based on allele frequency and sequencing depth of somatic mutations in tumor tissue and paired PLF samples. MAF: mutant allele frequency;  $\bar{x}_t$ : MAF in solid tumor tissue;  $\bar{x}_c$ : MAF in corresponding peritoneal lavage fluid (PLF);  $\bar{d}$ : sequencing depth in PLF;  $\bar{m}$ : mutation reads number in PLF;  $\bar{p}$ : observing reads with mutation in PLF; and R: overall cancer cell concentration. (b). The linear

correlation between theoretical and estimated cancer cell fraction up to the dilution of 1:10<sup>-5</sup>. Each dilution was repeated three times. The blue dots highlight the fractions above the limit of detection (PLC/PRF/5 cell fraction = 0.001%, 0.005%, 0.05%, 0.5%, 5% and 33%). The red dots highlight the fractions under the limit of detection (PLC/PRF/5 cell fraction = 0.0001%, 0.0003%). (c). Background noise observed in the cancer cell fraction model at 0% PLC/PRF/5 cell input among the 20 independent replicates (green dots). Experiments performed on different cell line dilutions (0.0001% and 0.0003%, red dots; 0.001%, blue dots) were repeated three times. (d). Biological noise of the 104 PLF samples from patients. The cancer cell fraction for each sample was calculated based on non-tumor-specific mutations.

a



b

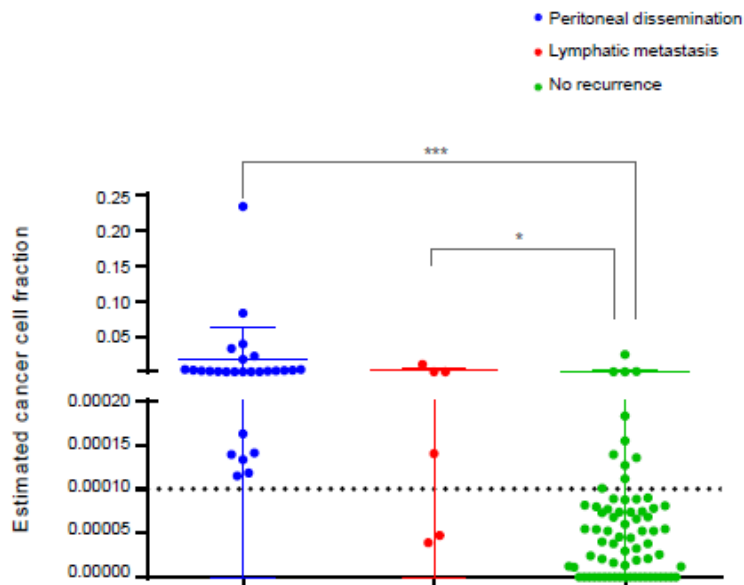


### Figure 3

Summary of clinical and histopathologic parameters, somatic mutations and cancer cell fraction for all patients. (a). Top panel, the summary of the frequencies of the tracked mutations in tumor and matched peritoneal lavage fluid samples from 104 patients. Blue bar, the tumor frequency of each tracked mutation. Frequency values are shown on the left vertical axis. Red bar, the detected peritoneal lavage fluid frequency of each tracked mutation. Frequency values are shown on the right vertical axis. The clinical outcome of patients is indicated under the bar. Middle panel, the summary of the cancer cell fractions for each patient. Bottom panel, clinical and histopathological characteristics. (b). The cancer cell fraction distribution in patients with peritoneal dissemination (n = 27), lymphatic metastasis (n = 6) or no recurrence (n = 71). Reported p values are computed using 2-tailed Wilcoxon Mann-Whitney U test. \*\*\*, p < 0.001; \*, p < 0.05

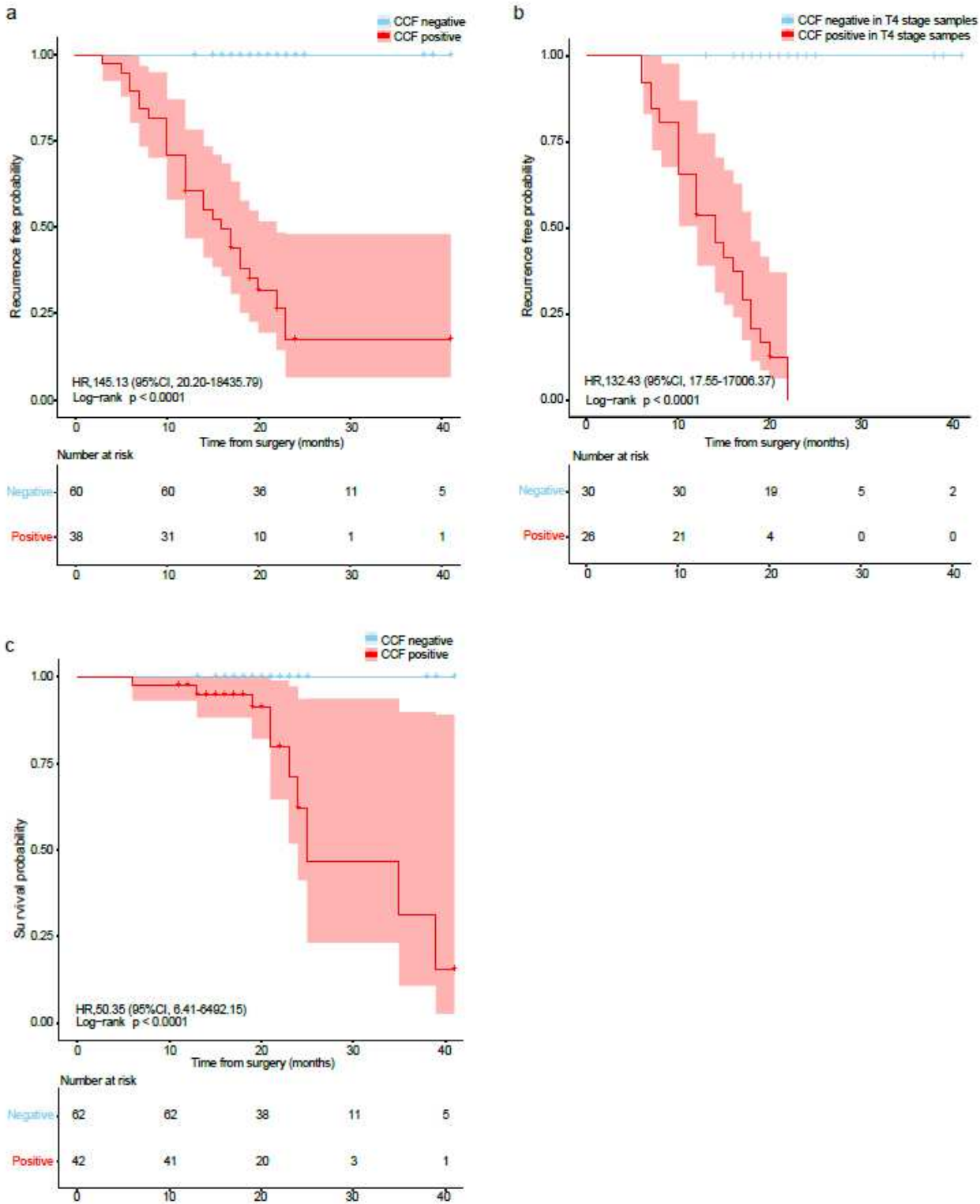


**Figure 4**

Kaplan-Meier estimates of recurrence-free survival (RFS) and overall survival (OS) for gastric cancer patients. (a) and (b). Kaplan-Meier survival analysis shows probability of recurrence-free survival (RFS) as determined by A. cancer cell fraction detected in peritoneal lavage fluid ( $n = 98$ ); and B. cancer cell fraction detected in peritoneal lavage fluid in stage T4 patients ( $n = 56$ ) (for peritoneal dissemination). A patient was classified as testing positive if the cancer cell fraction detected in peritoneal lavage fluid was

> 0.01%; (c) Kaplan-Meier estimates of overall survival (OS) for 104 gastric cancer patients based on the estimated cancer cell fraction in peritoneal lavage fluid. Shaded areas in the Kaplan-Meier plots indicate 95% CIs. HR: hazard ratio; CCF: cancer cell fraction.

## Supplementary Files

This is a list of supplementary files associated with this preprint. Click to download.

- [SupplementaryFigures.pdf](#)
- [SupplementaryTables.xlsx](#)